Sound & Vibration 2025, 59(1), 1702.
https://doi.org/10.59400/sv1702

Article

Coupled Helmholtz resonators for broadband Aeroacoustic noise mitigation

Zixiang Xiong[1], Xuxu Zhuang[1], Zhaoyong Sun[2], Liuxian Zhao[1,*]

[1] Institute of Sound and Vibration Research, Hefei University of Technology, 193 Tunxi Road, Hefei 230009, China
[2] Beijing Institute of Graphic Communication, 1 Xinghua Avenue (Band 2), Beijing 102600, China
*** Corresponding author:** Liuxian Zhao, lxzhao@hfut.edu.cn

CITATION

Xiong Z, Zhuang X, Sun Z, Zhao L. Coupled Helmholtz resonators for broadband Aeroacoustic noise mitigation. Sound & Vibration. 2025; 59(1): 1702. https://doi.org/10.59400/sv1702

ARTICLE INFO

Received: 6 September 2024
Accepted: 12 October 2024
Available online: 18 December 2024

Abstract: As a structurally simple acoustic element, Helmholtz resonators can exhibit strong resonance when acoustic waves enter the cavity, thus providing excellent sound absorption effects. Consequently, they are widely applied in automotive engine and exhaust systems. This paper systematically investigates the noise reduction performance of multiple coupled Helmholtz resonators under conditions with and without tangential flow. A finite element simulation model with multiple Helmholtz resonators is established by employing COMSOL Multiphysics software to solve the linearized Navier-Stokes equations in the frequency domain. The simulation results demonstrate that the structure, which couples multiple Helmholtz resonators, can effectively broaden the low-frequency sound absorption band under the influence of a flow field, enhancing the transmission loss across the entire low-frequency band. This structure holds significant potential for applications in automotive exhaust systems and aero-engine noise reduction.

Keywords: Aeroacoustic noise; Helmholtz resonators; transmission loss; low-frequency absorption

1. Introduction

The invention of the automobile has dramatically facilitated people's travel and the transportation of goods. As times continue to evolve and people's pursuit of quality of life increases, there is a growing concern about the environmental noise pollution caused by automobiles. Studies have shown that the noise generated by the exhaust system accounts for about one-third of the total vehicle noise [1], making the reduction of exhaust noise particularly important in overall vehicle noise reduction. Exhaust noise is produced by the movement of fluids [2], usually stemming from the design of the engine camshaft, valve structure, and cylinder head. Still, changes in these areas can significantly affect the performance of the car engine, requiring continuous experimental verification, which is cumbersome and costly. In contrast, control at the periphery of the noise source is more direct and effective, and using exhaust silencers is one of the main methods. Exhaust silencers can effectively reduce noise in specific frequency bands, so developing high-quality silencers is the most essential part of the noise reduction process in the exhaust system [3,4]. Research on them significantly controls vehicle noise and urban traffic noise pollution.

The Helmholtz resonator is a type of resonator connected to the main pipe through a neck tube from a cavity, and it is also one of the components in silencers. The structure of Helmholtz resonator is relatively simple; the air inside the cavity acts like a spring, and the air in the neck area of the Helmholtz resonator acts like a mass block [5], thus forming an acoustic vibration system within the pipeline [6]. The traditional Helmholtz resonator is widely used for suppressing narrowband low-

frequency noise. Since the noises from the exhaust of cars are typically dominated by low frequencies, coupled Helmholtz resonators can significantly broaden the frequency range of the noise reduction.

In recent years, numerous researchers have conducted extensive studies on Helmholtz resonators and other types of silencers. In contrast to the standard Helmholtz resonator, Zhang et al. [7] suggested acoustic structure made of Helmholtz resonators lined with porous material, in which the porous lining assumes the embedded neck's predominant function in the system's energy dissipation. In order to achieve the optimal spatial utilization efficiency of Helmholtz resonators for the necessary noise reduction targets, Bi et al. [8] established theoretical models for both a single and multiple parallel Helmholtz resonators, as well as spatially divided cylindrical sound-absorbing bodies and grouped cavities. Li et al. [9] combined Helmholtz resonators with microperforated plates and achieved multiple resonances by dividing the gas cavities into unequal volumes. The experimental results showed that the proposed sound-absorbing material has a wider absorption bandwidth compared to traditional micro-perforated plate sound-absorbing materials. Yang et al. [10] introduced variable modular nested Helmholtz resonators that can control the quantity of sound absorption peaks by increasing or lowering the amount of nested resonators. This feature is advantageous for mitigating various narrowband disturbances that are not constant. Pan et al. [11] coupled two Helmholtz resonators with a pipe, with the two resonators sharing the same perforated sidewall, a structure that broadens the resonant frequency of the resonator. Mahesh and Mini [12] studied the normal incidence sound absorption characteristics of Helmholtz resonators with different structural forms from three aspects: theoretical analysis, numerical simulation, and experimental research, comparing the differences in sound absorption coefficients and resonant frequencies between multiple resonators in parallel and series configurations. Liu et al. [13] introduced a novel concept of using gradient perforated porous materials with Helmholtz resonators as backing. The gradient perforation technique greatly enhances the impedance matching between the material and air, resulting in improved sound absorption performance across a wide range of frequencies. The presence of a Helmholtz resonator on the backside results in an increase in sound absorption at low frequencies, hence boosting the overall sound absorption capability. This allows for a mix of low-frequency and wide-ranging sound absorption. Hoppen et al. [14] inserted a vibrating cantilever into the conventional Helmholtz resonator and compared it to a non-coupled Helmholtz resonator. The coupled resonator showed improved sound insulation efficiency and exhibited a second resonance frequency.

This paper uses the finite element simulation method to investigate the broadband aeroacoustic noise reduction performance of a system based on coupled Helmholtz resonators. Modeling and simulation are conducted with the COMSOL Multiphysics software to obtain the acoustic transmission loss of one, two, and four Helmholtz resonators under conditions with and without tangential flow.

2. Structural design and theoretical model

2.1. Structural design

To investigate the sound absorption performance of the silencer, a simulation model was established in COMSOL Multiphysics software, The numerical model geometry was referred to Emel Selamet's paper [15], and the original model was improved by adding three resonance cavities with different neck diameters to have more resonance peaks for enhancing the low-frequency acoustic absorption performance. **Figure 1** illustrates a schematic of the improved Helmholtz resonator in different quantities. The geometric structure consists of a cylindrical main pipe and one, two, and four cylindrical Helmholtz resonators on the sides. The air domain of the coupled Helmholtz resonator and the pipe was established within the model, with perfectly matched layers (PML) defined on both sides of the model to eliminate the impact of reflected waves. A background sound field was also set up at the pipe's entrance, generating a plane wave on the model's left side. The plane wave is defined as follows:

$$p_b = p_{in} \cdot e^{-ik_0 z} \tag{1}$$

$$k_0 = \frac{\omega}{c_0 + U_{in}} \tag{2}$$

$$V_b = (0,0,-\frac{1}{i\omega\rho_0} \cdot \frac{\partial p_b}{\partial z}) \tag{3}$$

where p_b is background sound pressure, p_{in} is the incident field sound pressure, defined as 1 Pa in this study, V_b is the background sound velocity vector, k_0 is the number of waves in the air, c_0 is the sound velocity in the air, U_{in} is the tangential flow velocity, ρ_0 is the air density.

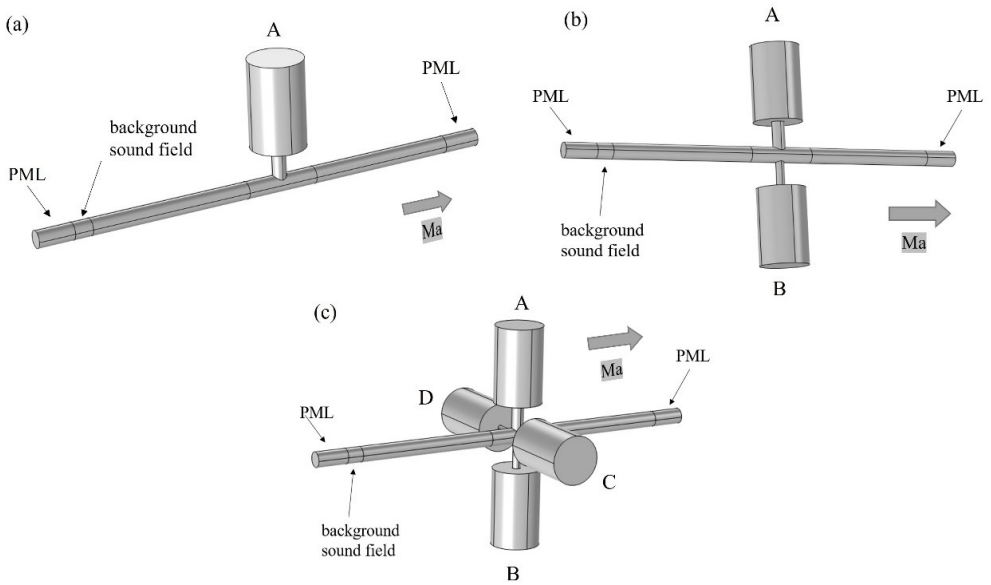

Figure 1. The models of Helmholtz resonators: **(a)** one HR; **(b)** two HRs; **(c)** four HRs.

The following equation determines the TL (Transmission Loss) of a piping system with a resonator:

$$TL = 20 * log_{10}(\frac{p_{in}}{p_{out}}) \tag{4}$$

where p_{out} is the surface-averaged sound pressure at the exit boundary.

In the flow context, a uniform steady-state flow is introduced from the left side and exits to the right side. The cylindrical Helmholtz resonators, designated as A, B, C, and D, are characterized by identical heights and diameters for the resonator cavity. Only the diameter of the necks of resonators is adjusted. This is because the change in neck diameter only affects a small portion of the resonator geometry and does not involve the volume or shape of the entire resonator, which results in less change to the overall geometry of the model, thus simplifying the model tuning process, and a slight adjustment of the neck diameter can significantly change the frequency range of the noise absorption. The specific dimensions and parameters of the Helmholtz resonators are detailed in **Table 1**. Where L_{PML} is the length of the perfectly matched layer in the pipe, L_B is the length of the background acoustic field in the pipe, L_{main} is the length of the pipe (excluding the length of the PML layer pipe and the length of the pipe in the background acoustic field), L_{neck} is the length of the resonator neck, L_{cav} is the height of the resonator cavity, D_{main} is the diameter of the main pipe, D_A,D_B,D_C, and D_D are the diameters of the necks of the four resonators, correspondingly, D_{cav} are the diameters of the resonators cavity, p_0 is the atmospheric pressure, and T_0 is the air temperature.

Table 1. Geometric dimensions of the coupled Helmholtz resonators.

Parameters	Values	Parameters	Values	Parameters	Values
L_{PML}	10.00 cm	D_{main}	4.859 cm	D_{cav}	15.32 cm
L_{main}	130.00 cm	D_A	4.044 cm	c_0	343 m/s
L_B	5.00 cm	D_B	2.696 cm	ρ_0	1.2 kg/m^3
L_{neck}	8.05 cm	D_C	2.022 cm	p_0	101,325 Pa
L_{cav}	24.42 cm	D_D	1.618 cm	T_0	297 K

2.2. Theoretical model

The Viscosity and compressibility of airflow are obtained by solving the linearized Navier-Stokes equations. The governing equations encompass the conservation of mass, momentum, and energy. Expressed within the Cartesian coordinate system, these equations are expressed as:

$$\frac{D\rho}{Dt} + \rho\frac{\partial u_k}{\partial x_k} \equiv 0 \tag{5}$$

$$\rho\frac{Du_i}{Dt} = -\frac{\partial p}{\partial x_i} + \frac{\partial \tau_{ij}}{\partial x_j} + \rho F_i \tag{6}$$

$$\rho\frac{De}{Dt} = -p\frac{\partial u_k}{\partial x_k} + \Phi + \frac{\partial}{\partial x_k}(\kappa\frac{\partial T}{\partial x_k}) \tag{7}$$

The shear stress equation is as follows:

$$\Phi = \tau_{ij}\frac{\partial u_i}{\partial x_j}, \tau_{ij} = \mu(\frac{\partial u_i}{\partial x_j} + \frac{\partial u_j}{\partial x_i} - \frac{2}{3}\frac{\partial u_k}{\partial x_k}\delta_{ij}) \tag{8}$$

where D/Dt is the convective conductivity, u_i is the velocity component in the ith direction, τ_{ij} is the viscous stress tensor, F_i is the volume force in the ith direction, Φ is the dissipation function, δ_{ij} is the Kronecker function and uses the Einstein summation convention, κ is the thermal conductivity, μ is the dynamic viscosity, $p = \rho RT$, ρ is the density, R is the gas constant divided by molecular weight, T is the absolute temperature, $e = e(p, T)$, and e is the internal energy.

Each flow parameter in the pipeline consists of average and fluctuating values as follows:

$$\begin{cases} \rho(x,t) = \rho_0(x) + \rho'(x,t) \\ u(x,t) = u_0(x) + u'(x,t) \\ v(x,t) = v_0(x) + v'(x,t) \\ p(x,t) = p_0(x) + p'(x,t) \end{cases} \tag{9}$$

The first component on the right-hand side of Equation (9) corresponds to the average flow, whereas the second term indicates the flow disturbance. It is believed that the perturbation flow is a harmonic function of time and may thus be converted into the frequency domain. Since the model incorporates the average flow in the pipeline, it is necessary to choose a suitable turbulence model. The Shear Stress Transport (SST) turbulence model, introduced by Menter [16] in 1994, is extensively employed in engineering as one of the most popular turbulence models. The SST model integrates two distinct turbulence models: the $k-\omega$ model is employed in the boundary layer region, while the $k-\varepsilon$ model is utilized in the free flow zone. Moreover, the SST model exhibits reduced numerical diffusion, allowing for precise prediction of turbulence across different flow conditions.

3. Result and discussion

3.1. Ignoring the impact of fluid dynamics on the Helmholtz resonator

First, let us analyze the case when the tangential flow Mach number is 0, i.e., without considering the effect of the flow field on the Helmholtz resonators. **Figure 2** shows the transmission loss from 0 to 200 Hz for the three models of one, two, and four Helmholtz resonators at Ma = 0. The resonance frequency of the Helmholtz resonator depends on its geometry [17,18], and the resonance frequency is $f = \frac{c}{2\pi}\sqrt{\frac{A}{VL'}}$, where c is the velocity of acoustic wave propagation in air, A is the cross-sectional area of the resonator neck, V is the volume of the cavity, and L' is the end-corrected neck length. Since the sound wave does not abruptly stop at the neck, but rather extends a short distance, increasing the actual acoustic effective length, the neck length of the Helmholtz resonator needs to be corrected toL', $L' = L + 2\delta_R$ [19], where $\delta_R \approx 0.6d$ [20], L is the length of the resonator neck and d is diameters of the necks.

To validate the effectiveness of the simulation model used in this study, we selected the simulation and experimental data from reference [15] for comparison. Reference [15] utilized similar geometric dimensions and boundary conditions, and its model closely resembles the single Helmholtz resonator structure investigated in this study. Therefore, it serves as a valid reference for comparison. A comprehensive comparison shows that at Ma = 0, the simulation results for the single Helmholtz resonator are in good agreement with both the experimental and simulation results from reference [15]. Additionally, the trend of transmission loss as a function of frequency is consistent with that reported in reference [15].

It can be observed that the resonant frequency is 89Hz of resonator A from **Figure 2**. Although the maximum transmission loss is 45dB, the absorption bandwidth is relatively narrow. When an additional resonator B with a smaller diameter of neck is added, a resonant peak at 61Hz appears, and an additional absorption bandwidth is observed. Upon further addition of resonators C and D with even smaller diameter of necks, resonant peaks at 37Hz and 46Hz are observed, resulting in four absorption bands. **Figures 3**–**5**, respectively, illustrate the sound pressure distributions at the four resonant peak frequencies for one, two, and four Helmholtz resonators. It is evident from **Figure 3** that the sound pressure distribution at 89Hz for a single resonator is significantly lower than at other frequencies. The same is true for the cases with two (**Figure 4**) and four resonators (**Figure 5**), where excellent sound absorption performance is observed at their respective resonant frequencies. Therefore, it can be concluded that when the tangential flow Mach number is 0, as the number of Helmholtz resonators increases from one to four, the absorption bands in the 0~200Hz frequency range are noticeably risen from one to four. However, these absorption bands are discontinuous and relatively narrow, making it challenging to achieve broadband sound absorption and noise reduction effects.

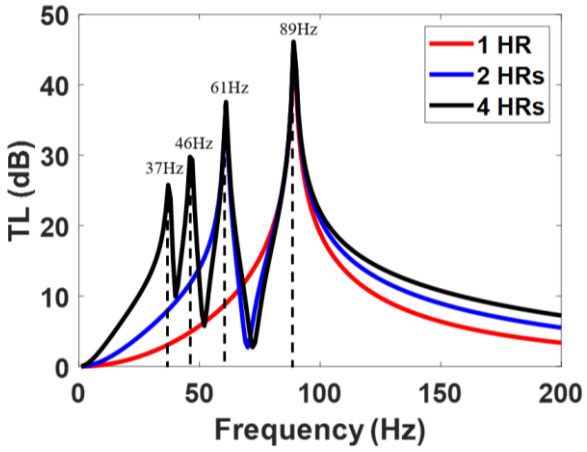

Figure 2. Transmission loss in the f = 0~200 Hz band for the three models at Ma = 0.

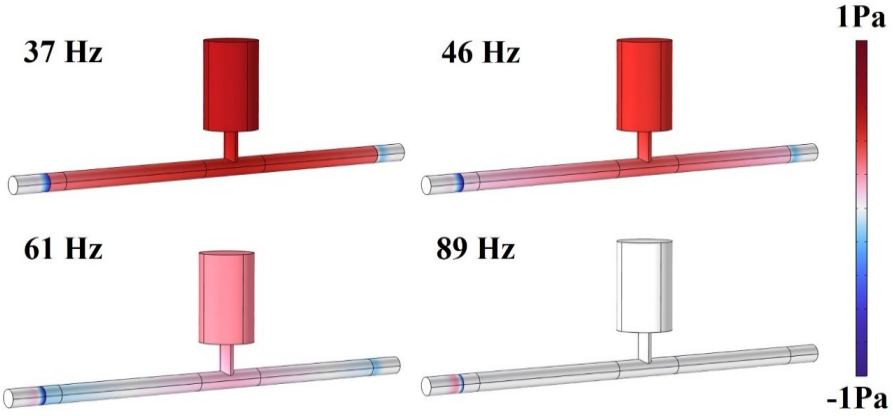

Figure 3. Sound pressure distributions at four resonant peak frequencies (one HR).

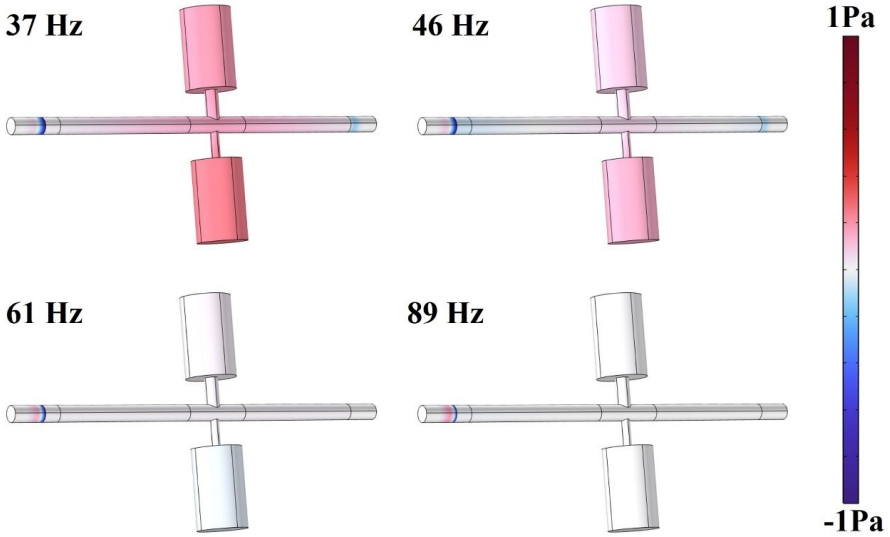

Figure 4. Sound pressure distributions at four resonant peak frequencies (two HRs).

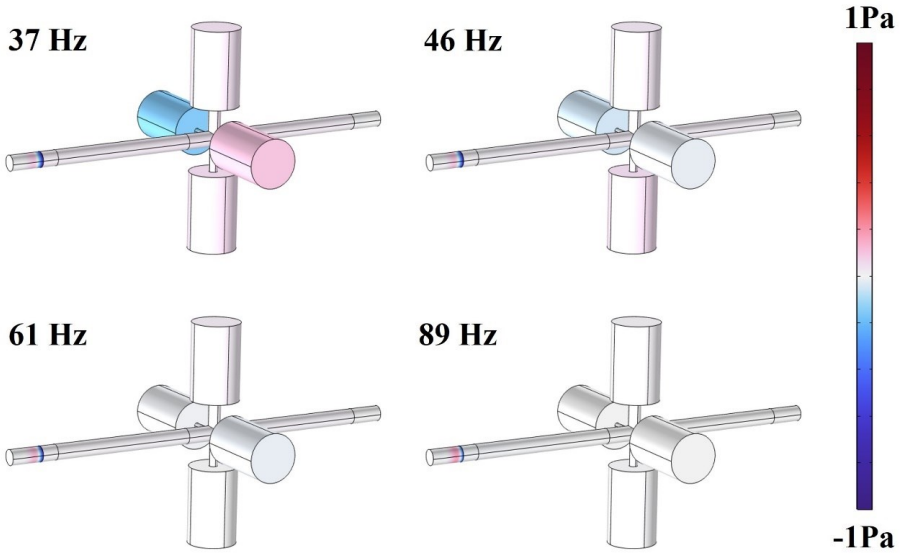

Figure 5. Sound pressure distributions at four resonant peak frequencies (four HRs).

3.2. Considering the effect of flow on Helmholtz resonators

When coupling the model with Helmholtz resonators and considering the interaction between the flow field and the acoustic field, COMSOL Multiphysics software is used for modeling and simulation. Initially, a Computational Fluid Dynamics (CFD) model must be established to calculate the flow at different tangential flow Mach numbers. Subsequently, after the completion of the CFD model calculation, the solution obtained from the CFD mesh is mapped to the acoustic mesh through the background fluid flow coupling. Finally, after establishing the acoustic model, the mapped flow field is used as input to solve the linearized Navier-Stokes equations under the influence of the tangential flow.

Figure 6 presents the transmission loss in the 0–200Hz range for models with one, two, and four Helmholtz resonators at Ma = 0.05. The Reynolds number range is 1.86×10^4~4.65×10^4. When the tangential flow Mach number is 0.05, the resonant peak frequencies of the three models with coupled Helmholtz resonators are slightly shifted to the right compared to the resonators without considering the flow field effect. When airflow passes through a Helmholtz resonator, the velocity of the airflow alters the propagation characteristics of sound waves. The Strouhal number describes this change by relating the frequency to the flow velocity. As the airflow velocity changes, the resonant frequency correspondingly shifts to maintain an approximately constant Strouhal number. At low velocity flows, the Strouhal number usually remains at an approximately constant value, so that the resonance frequency is linearly related to the flow velocity. That is, as the flow velocity increases, the resonance frequency increases accordingly. The noise reduction bands become wider and continuous, but the transmission loss is reduced. This is due to the interaction between the flow field and the acoustic field, which causes changes in sound attenuation and propagation . As the number of coupled Helmholtz resonators increases, the noise reduction frequency bands in **Figure 6** can be seen to be widen gradually, and the transmission loss increases across the entire frequency band.

Figure 7 shows the transmission loss in the 0–200Hz range for models with one, two, and four Helmholtz resonators when the tangential flow Mach number is 0.1. The Reynolds number range is 3.72×10^4~9.3×10^4. As the tangential flow Mach number increases, although the transmission loss of multiple coupled Helmholtz resonators may decrease, they can still achieve broadband aeroacoustic noise suppression in the low-frequency range.

Through the comparison of **Figures 6** and **7** with the data results in the reference [15], it is found that the simulation results of a single Helmholtz resonance cavity in this paper also coincide with the experimental and simulation results and the change trend in the reference [15], which once again illustrates the validity of the simulation in this paper.

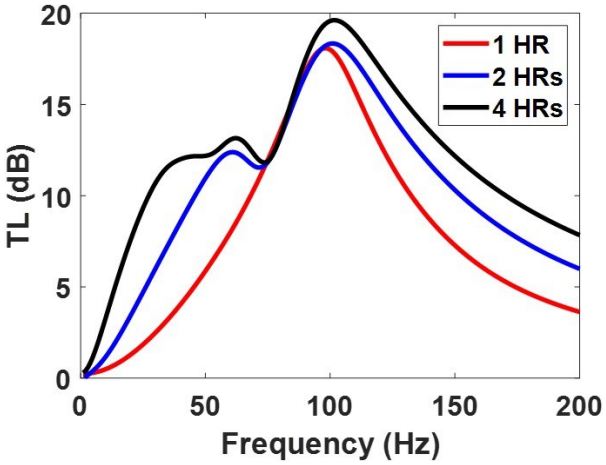

Figure 6. Transmission loss in the f = 0~200 Hz band for the three models at Ma = 0.05.

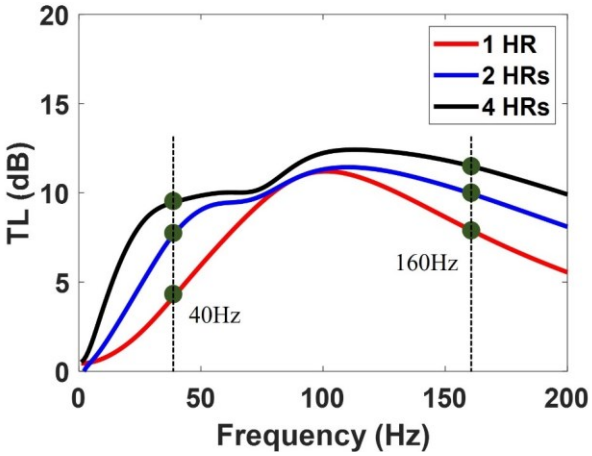

Figure 7. Transmission loss in the f = 0~200 Hz band for the three models at Ma = 0.1.

This study investigates the differences in sound pressure distribution at the same frequency for one, two, and four coupled Helmholtz resonators at Ma = 0.1. To make the differences more pronounced, the frequencies of 40Hz and 160Hz, which have a significant difference in transmission loss (as shown in **Figure 5**), were selected for the study. **Figure 8** illustrates the sound pressure distribution of the three coupled Helmholtz resonator models at 40Hz and 160Hz. At these frequencies, the sound pressure at the pipe outlet decreases significantly with the increase of the number of coupled Helmholtz resonators. This implies that the transmission loss decreases as the number of coupled Helmholtz resonators increases. **Figure 9** shows the background mean velocity distribution for the three Helmholtz resonator models. It can be observed that as the number of resonators increases, the fluid flow characteristics of the entire system change significantly, particularly near the necks of the resonators. The greater the number of resonators, the more pronounced the disturbance to the flow field. Therefore, we can conclude that a silencer coupling multiple Helmholtz resonators with different neck diameters can effectively broaden the low-frequency absorption frequency band with the influence of tangential flow. Compared to a

silencer coupled with a single Helmholtz resonator, it can enhance the overall transmission loss in the low-frequency band.

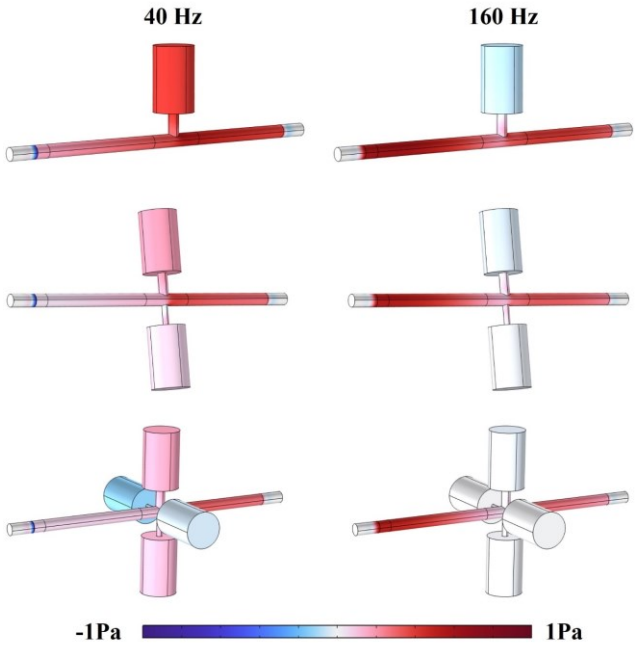

Figure 8. Sound pressure distributions at four resonant peak frequencies of the three Helmholtz resonant models.

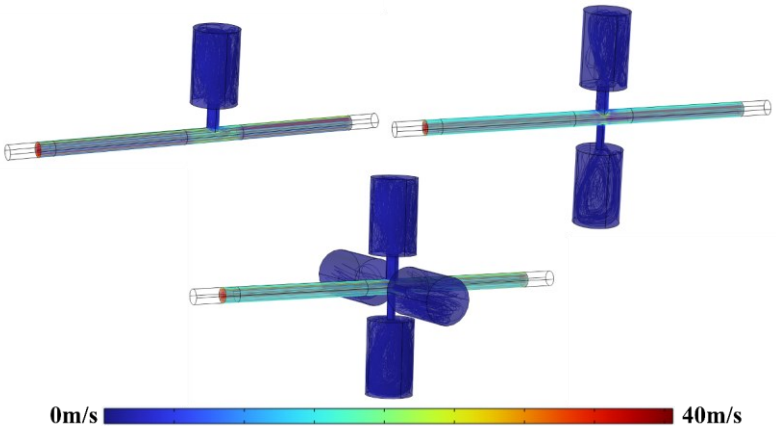

Figure 9. Background mean flow velocity distribution at Ma = 0.1.

4. Conclusion

This paper presents a coupled model of multiple Helmholtz resonators under the condition of tangential flow and investigates its broadband low-frequency sound absorption performance through numerical simulation methods.

By establishing a finite element simulation model with multiple Helmholtz resonators using the finite element software COMSOL Multiphysics and solving the linear Navier-Stokes equations in the frequency domain, the results indicate that the silencer coupling multiple Helmholtz resonators with different neck diameters can significantly enhance the transmission loss in the f = 0~200Hz frequency range and broaden its low-frequency absorption band compared to a single Helmholtz resonator.

This research outcome provides a reference for the design of silencers with flow field effects and offers new insights into the aeroacoustic research of the coupled model of Helmholtz resonators.

Author contributions: Conceptualization, ZX and LZ; methodology, ZX and LZ; software, ZX; validation, ZX, XZ, ZS and LZ; resources, LZ; data curation, ZX and LZ; writing—original draft preparation, ZX; writing—review and editing, ZX, XZ, ZS and LZ; funding acquisition, LZ. All authors have read and agreed to the published version of the manuscript.

Data availability: The data that support the findings of this study are available from the corresponding author upon reasonable request.

Funding: The authors sincerely acknowledge the financial support of the National Natural Science Foundation of China (Grant No. 12474462), and Anhui Provincial Natural Science Foundation (Grant No. 2308085ME162).

Conflict of interest: The authors declare no conflict of interest.

References

1. Feng XN. Optimization research on vibration and noise of exhaust system of a model[D]. Hunan University, 2020.
2. Li C, Wang X, Li Y. Experimental study on aerodynamic noise characteristics and control of non-fully open low-speed cavities[J]. Applied Acoustics, 2023, 212: 109600.
3. Zhao L, Lam Y C, Lai C Q. Interaction of ultrasound with microporous polyethylene scaffolds[J]. Applied Acoustics, 2019, 153: 102–109.
4. Zhao X, Liu Y, Zhao L, et al. A scalable high-porosity wood for sound absorption and thermal insulation[J]. Nature Sustainability, 2023, 6(3): 306–315.
5. Sheng M, Wang M Q, Sun J C. Fundamentals of Noise and Vibration Control Technology [M]. Beijing: Science Press, 2007.
6. Jena D P, Dandsena J, Jayakumari V G. Demonstration of effective acoustic properties of different configurations of Helmholtz resonators[J]. Applied Acoustics, 2019, 155: 371–382.
7. Zhang W, Xin F. Broadband low-frequency sound absorption via Helmholtz resonators with porous material lining[J]. Journal of Sound and Vibration, 2024, 578: 118330.
8. Bi S, Wang E, Shen X, et al. Enhancement of sound absorption performance of Helmholtz resonators by space division and chamber grouping[J]. Applied Acoustics, 2023, 207: 109352.
9. Li H, Wu J, Yan S, et al. Design and study of broadband sound absorbers with partition based on micro-perforated panel and Helmholtz resonator[J]. Applied Acoustics, 2023, 205: 109262.
10. Yang X, Shen X, Yang F, et al. Acoustic metamaterials of modular nested Helmholtz resonators with multiple tunable absorption peaks[J]. Applied Acoustics, 2023, 213: 109647.
11. Pan W, Xu X, Li J, et al. Acoustic damping performance of coupled Helmholtz resonators with a sharable perforated sidewall in the presence of grazing flow[J]. Aerospace Science and Technology, 2020, 99: 105573.
12. Mahesh K, Mini R S. Investigation on the Acoustic Performance of Multiple Helmholtz Resonator Configurations[J]. Acoustics Australia, 2021, 49(2): 355–369.
13. Liu H, Wang J, Zhang X, et al. Research on the Generation Mechanism and Suppression Method of Aerodynamic Noise in Expansion Cavity Based on Hybrid Method[J]. Computer Modeling in Engineering & Sciences, 2024, 139(3): 2747–2772.
14. Hoppen H, Langfeldt F, Gleine W, et al. Helmholtz resonator with two resonance frequencies by coupling with a mechanical resonator[J]. Journal of Sound and Vibration, 2023, 559: 117747.
15. Selamet E, Selamet A, Iqbal A, et al. Effect of Flow on Helmholtz Resonator Acoustics: A Three-Dimensional Computational Study vs. Experiments[C]//SAE 2011 Noise and Vibration Conference and Exhibition. 2011: 2011-01-1521.
16. Menter F R. Two-equation eddy-viscosity turbulence models for engineering applications[J]. AIAA Journal, 1994, 32(8): 1598–1605.

17. Dandsena J, Jena D P. Acoustic attenuation and effective properties of single and periodic Helmholtz resonators having porous core[J]. Applied Acoustics, 2023, 211: 109490.
18. Papadakis N M, Stavroulakis G E. FEM Investigation of a Multi-Neck Helmholtz Resonator[J]. Applied Sciences, 2023, 13(19): 10610.
19. Pagliaroli T. Wall pressure fluctuations in rectangular partial enclosures[J]. Journal of Sound and Vibration, 2015.
20. Rayleigh, John William Strutt, Baron, Lindsay, Robert Bruce. The theory of sound[M].Dover Publications, 1945.